

# Routing in ZigBee: benefits from exploiting the IEEE 802.15.4 association tree

Francesca Cuomo, Sara Della Luna, Ugo Monaco  
University of Roma "La Sapienza", INFOCOM Dept.  
Via Eudossiana 18, 00184, Rome, Italy  
{cuomo,monaco}@infocom.uniroma1.it,  
dellaluna@net.infocom.uniroma1.it

Tommaso Melodia  
Broadband and Wireless Networking Laboratory  
Georgia Institute of Technology, Atlanta, Georgia 30332  
tommaso@ece.gatech.edu

**Abstract**— An IEEE 802.15.4-based Wireless Sensor Network is considered, and the relationship between the IEEE 802.15.4 topology formation mechanism and possible routing strategies at the network layer is studied. Two alternative routing schemes proposed in the framework of the ZigBee Alliance are analyzed. The first is the well-known Ad-hoc On demand Distance Vector (AODV) routing protocol, which was designed for highly dynamic application scenarios in wireless ad-hoc networks. The second is a tree-based routing scheme based on a hierarchical structure established among nodes during the network formation phase. This latter approach, referred to as HERA (HiErarchical Routing Algorithm) in the paper, routes packets from sensors to sink based on the parent-child relationships established by the IEEE 802.15.4 topology formation procedure.

An extensive simulation analysis is carried out to compare HERA and AODV. It is shown that a hierarchical routing scheme based on the MAC association procedures offers several benefits with respect to reactive routing in typical sensor network applications. Moreover, it is to be noted that most sensor network scenarios are concerned with delivery of packets from a series of static sensors to a single, static, sink.

## I. INTRODUCTION

The IEEE 802.15.4 group has recently proposed standard *physical* (PHY) and *medium access control* (MAC) layers [1] for Wireless Personal Area Networks (WPAN) optimized for low data rate applications (0.01 – 250 kbit/s) with simple or no quality of service (QoS) requirements. IEEE 802.15.4 is designed to wirelessly interconnect ultra low-cost sensors, actuators, and processing devices, which will constitute the infrastructure to sense and affect the physical environment [2][3]. Typical applications of IEEE 802.15.4 devices are envisioned to be: i) industrial control, ii) environmental and health monitoring; iii) home automation, entertainment and toys; iv) security, location and asset tracking; v) emergency and disaster response.

With respect to previous WPAN standards such as Bluetooth [4], the IEEE 802.15.4 standard is characterized by lower power consumption and lower cost [5]. While, in line with the family of IEEE 802 standards, the proposal focuses only on PHY and MAC layers, upper layers of the protocol stack are defined by the ZigBee Alliance [6], which also deals with marketing and interoperability of WPAN devices from different manufacturers. In a relationship which is similar to that between IEEE 802.11 and the Wi-Fi alliance, ZigBee has

devised a specification [7] for a suite of high-level communication protocols based on IEEE 802.15.4.

IEEE 802.15.4 can operate at data rates of 250 kbit/s at 2.4 GHz, 40 kbit/s at 915 MHz (North America), and 20 kbit/s at 868 MHz (Europe). While the data rate is much lower than Bluetooth, the energy consumption is at least one order of magnitude lower and recent low-cost commercial versions have demonstrated the viability of this technology for low duty cycle (< 0.01) sensor applications. Significantly, the latest generations of motes from Crossbow [8], i.e., MICAz [9] and TELOS [10], are based on the first IEEE 802.15.4 compliant Chipcon CC2420 radio [11].

In this paper, we consider an IEEE 802.15.4-based Wireless Sensor Network (WSN) and we study the relationship between the IEEE 802.15.4 topology formation mechanism and possible routing strategies at the network layer. Our objective is to explore the cross-layer interdependencies between the topology formation and routing mechanisms to set-up energy-efficient routing paths towards a sink.

To this aim, we evaluate the behavior of two alternative routing schemes that have been proposed in the framework of the ZigBee Alliance as possible alternatives for IEEE 802.15.4 sensor networks. The first is the well-known Ad-hoc On demand Distance Vector (AODV) routing protocol [12], which was designed for highly dynamic application scenarios. The second is a simple hierarchical routing scheme, which we refer to as HiErarchical Routing Algorithm (HERA). HERA routes packets from sensors to sink based on the parent-child relationships established by the IEEE 802.15.4 MAC topology formation procedure. The two schemes are inherently different, as the former is a pure on-demand route acquisition algorithm that broadcasts discovery packets when a routing path needs to be established, while the latter is a proactive routing scheme that does not use *ad hoc* control messages.

The purpose of this research is to assess and compare the performance of these two alternative routing strategies and to highlight the main strengths and drawbacks of these schemes. To the best of our knowledge, this is the first paper to deal with this topic in the framework of the IEEE 802.15.4 standard.

We carried out an extensive simulation analysis to compare HERA and AODV. We show that a hierarchical routing scheme based on the MAC association procedures offers several ben-

efits in sensor network applications such as:

- it exploits information exchanged during the network formation and topology update phases, thus avoiding additional routing messages and the associated overhead;
- it shows performance benefits with respect to AODV, such as reduced latency and energy consumption, in practical application scenarios;
- it reduces complexity, as it is very easy to implement and does not require a specialized daemon on the host device where it runs.

The remainder of the paper is organized as follows. Section II introduces the IEEE 802.15.4 association procedures. Section III describes the hierarchical routing scheme, HERA. Then, the performance analysis framework is reported in Section IV, while the performance comparison between HERA and AODV is discussed in Section V. Finally, Section VI outlines the main conclusions.

## II. OVERVIEW OF IEEE 802.15.4 AND ZIGBEE

An IEEE 802.15.4 WPAN is composed of a PAN coordinator and a set of devices. The PAN coordinator is the primary controller of the network. It is responsible for initiating network operations, and may be mains powered. According to their capabilities and available resources, IEEE 802.15.4 devices can be full-function devices (FFD) or reduced-function devices (RFD). In [1], a set of procedures is defined to allow the PAN coordinator to start a new WPAN, and to allow devices to join this WPAN. The procedures to establish and maintain device membership in a WPAN are named *association procedure* and *realignment procedure*, respectively [1].

### A. Association Procedure

The operations accomplished by a device to join a WPAN can be summarized as follow: *i)* scan for available WPANs; *ii)* select the WPAN to join; *iii)* start the association procedure with the PAN coordinator or with another device that has already joined the WPAN, named simply coordinator.

The discovery of available WPANs is performed by scanning *beacon frames* broadcast by a PAN coordinator or by other coordinators. Two possible ways of broadcasting beacons are defined in the standard: *beacon-enabled* and *nonbeacon-enabled* mode. In beacon-enabled mode, beacon frames are periodically transmitted and all communications are performed through a superframe structure. A superframe is bounded by periodically transmitted beacon frames, which allow nodes to synchronize to the network. Therefore, two different types of scan are defined:

- 1) *Passive scan*: in *beacon-enabled networks* associated devices periodically transmit beacon frames, hence information on available WPANs can be derived by eavesdropping the wireless channel;
- 2) *Active scan*: in *nonbeacon-enabled networks* beacon frames are not periodically transmitted but need to be explicitly requested by means of a *beacon request command frame*.

After scanning the channel, a list of available WPANs is available at the scanning device, among which the network to connect to is to be chosen. Then, the device sends an association request to the PAN coordinator or to the device, named coordinator, through which the selected network was discovered. The association phase ends with a successful *association response command frame* to the requesting device, and the reception of this message establishes the synchronization between the requesting device and its coordinator. Hence, this procedure basically results in a set of MAC association relationship between devices, named in the following *parent-child relationship*. All these relationships form a tree rooted at the PAN coordinator.

### B. Realignment Procedure

The standard also describes a mechanism to maintain and re-associate a device with a coordinator in case of disconnections. In fact, due to the high variability of the wireless channel, limited power and possible mobility, a sensor node can lose synchronization with its coordinator, i.e., a certain number of beacon frames from the coordinator can be lost. In this case, the so-called *orphaned* device starts the realignment procedure, which consists of an *orphan scan* phase, which is aimed at re-establishing synchronization with the previous coordinator if this is still reachable. Otherwise, a new association procedure is triggered.

In [7], the ZigBee Alliance has defined network, security and application software layers for IEEE 802.15.4 devices. Basically, the application and security layers provide a framework for application support and security services, while the network layer mainly includes mechanisms for network topology setup and routing issues which are the main concerns of this work. In particular, the ZigBee network layer supports three different topologies: *i)* star, *ii)* tree or *iii)* mesh.

In the star topology, every device transmits packets directly to the ZigBee coordinator, i.e., the PAN coordinator, and direct transmissions between other devices are not allowed. In the tree topology, a tree rooted at the ZigBee coordinator is created based on the MAC parent-child relationships between IEEE 802.15.4 devices. In the tree topology case a hierarchical routing scheme can be implemented. Finally, in mesh topologies, direct transmissions between non parent-child devices is allowed. In this case, a reactive routing scheme based on a simplified version of AODV has been proposed. We remark that, even in mesh topologies, the parent-child tree structure is always created by the IEEE 802.15.4 MAC layer to start a new PAN, but this hierarchical tree structure is not used for routing purposes.

## III. HIERARCHICAL ROUTING ALGORITHM

In accordance to the ZigBee guidelines, we implemented a hierarchical routing (HERA) that takes advantage of the MAC layer associations to perform the routing functionality. With HERA, data generated by the sensors and directed to the

sink are routed downward to the root tree along the parent-child relationships, i.e., every node relays data to its parent. On the other hand, for sensor-to-sensor or sink-to-sensor communications, packets are routed upward or downward along the tree according to the address of the destination of the data by exploiting the hierarchical addressing scheme provided by ZigBee. This routing algorithm is proactive in the sense that routes towards the destination are resolved before a sensor node (also called node in the following) needs to perform packet routing. The resulting routing tree corresponds with the tree that is formed during the MAC association procedure, described in Section II, to create the IEEE 802.15.4 network. Therefore, routing paths are based on MAC *parent-child relationship* and result in a tree rooted at the ZigBee/PAN coordinator, e.g., the sink in a sensor network. Hence, to gather data generated by the sensors at the sink in a multi-hop network, each node shall transmit all the packets to its own IEEE 802.15.4 coordinator. More specifically, if we denote with:

- $n_0$  the sink node;
- $l$  the level of each node in the tree, so that a level- $l$  node is  $l$  hops far from  $n_0$  (with  $n_0$  being the only level-0 node);
- $n_i^l(p)$  the  $i$ -th child at level- $l$  associated with node  $p$  (at level  $(l - 1)$ );

then, every node  $n_i^l(p)$  routes all packets directed to the sink  $n_0$  toward its parent  $p$  (with  $p = n_0$  for level-1 nodes). We remark that the resulting routing paths do not change while synchronization between device and coordinator is maintained, and will be eventually updated after orphan scan calls, e.g., in case of loss of synchronization.

The HERA routing algorithm consistently reduces message exchange since it leverages MAC association procedures. It must be considered that these messages are exchanged anyway during the topology formation phase. A *cross-layer interaction* is thus exploited between routing and MAC. HERA turns out to be simple, light and does not require large memory for routing tables. These features make HERA a good candidate for routing in IEEE 802.15.4 WSNs. On the other hand, it must be noted that routing paths are not optimized with respect to any routing metric, e.g., hop count and bandwidth. However, because of the cross-layer nature of this routing strategy, routing optimization can be achieved by accurately designing the IEEE 802.15.4 association procedures, to create efficient routes according to a given optimization objective.

#### IV. PERFORMANCES ANALYSIS

##### A. Implementation of the HERA routing algorithm

To assess the performance of the proposed hierarchical routing scheme, we implemented HERA in ns-2 [13]. ns-2 includes implementations of the IEEE 802.15.4 physical and MAC layers [14], and of several routing protocols. In particular, we implemented the HERA algorithm by extending the NO Ad-Hoc (NOAH) routing agent [15], and by implementing a cross-layer interaction between link and routing layers to route

data packets to the coordinator with which each device has been successfully associated. The address of a coordinator is available at MAC layer in the *association response command frame* sent by coordinator to its child and it is forwarded to the network layer which inserts it in the routing table as next-hop for packets destined to the sink.

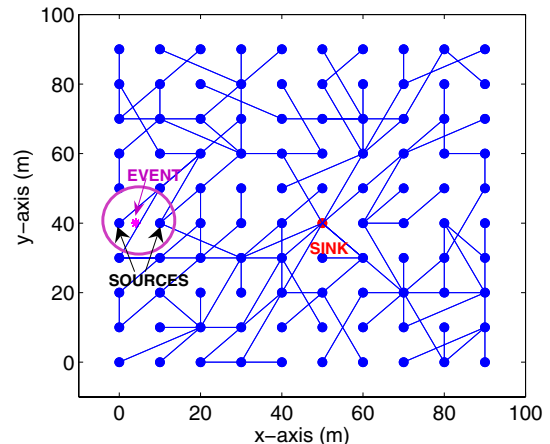


Fig. 1. Simulation scenario: black points represent sensor nodes and edges correspond to *parent-child relationships*

##### B. Topology Description and Simulation Scenarios

We consider a network consisting of  $N = 100$  sensor nodes distributed on a  $100 \times 100$  m grid (shown in Fig. 1). All sensors are FFD devices configured in nonbeacon-enabled mode, and they are all potential coordinators in the WPAN allowing for the association of other devices. We consider a single sink located around the center of the area ( $x_s = 50$  m and  $y_s = 40$  m). We further assume that an event happens in the monitored region (in Fig. 1, the event is centered at  $x_{eve} = 4$  m,  $y_{eve} = 40$  m), and that an event range  $R_{eve}$  models the maximum distance at which a sensor can detect the event. All sensors within  $R_{eve}$  of the event center, called in the following *source nodes*, generate data that shall be gathered at the sink, while the other sensors participate in the multi-hop relaying process, if necessary. The number of source nodes depends on the event range. The traffic generated by the source nodes is 1 packet/s for the entire duration of the event  $t_{eve}$ , while the MAC frame size is 40 bytes, which corresponds to an average generation data rate equal to 0.32 kbit/s.

We remark that once the PAN coordinator starts the WPAN, MAC associations established between devices depend on: i) the exact time at which each single device is turned on; ii) the radio transmission range. We considered a random inter-device switch on time  $t_s$ , with  $0 \text{ ms} \leq t_s \leq 10 \text{ ms}$ . Moreover, two different radio transmission ranges  $rTx = \{20 \text{ m}, 30 \text{ m}\}$ , are considered. If the distance between two devices is greater than  $rTx$ , transmitted frames are lost, while if the distance is lower than  $rTx$ , transmitted frames are successfully received. In this latter case, frame losses due to MAC collisions and interference are also taken into account by means of a capture

threshold ( $CPT_{thresh} = 10dB$ ) on the signal-to-interference ratio. From the topology in Fig. 1, it follows that if  $rTx = 20$  m a node has 8 neighbors, while  $rTx = 30$  m corresponds to 24 neighbors. In the considered scenario, all sensors have the same transmission range.

The performance analysis presented in the next section has been carried out by varying  $R_{eve}$  between 10 m and 40 m with step 5 m, which corresponds to a number of source nodes of 2, 6, 9, 13, 18, 26 and 31, respectively. Moreover, we considered two different event duration times, i.e., a short event with  $t_{eve1} = 60$  s and a long event with  $t_{eve2} = 500$  s. The node energy consumption for data transmission/reception during the simulation has also been taken into account. The initial value of the node energy level is set to  $E_0$ , and it is decremented for every transmission and reception of packets. When the energy level at the node reaches zero, the node dies. We set the transmitting and receiving power to  $0.0756W$  and  $0.0828W$ , respectively (as reported in [16] for some operational sensor devices). Finally, to assess the performance of the considered routing strategies in steady network conditions, we set  $E_0$  to prevent nodes from depleting their batteries during the simulation. Hence, network topology changes due to dead nodes do not occur for the whole duration of the simulation.

### C. Performance Metrics

We measure different performance metrics. In particular, for each source we evaluate:

- *End-to-End Delay*: the time interval between the transmission of the packet by a source node and the reception at the sink.
- *Packet Loss*: percentage of packets lost, as the ratio between the number of packets successfully received at the sink and all packets generated by the source node.
- *Number of RREQ*: number of route request control messages generated by sources to discover paths towards the sink (only for AODV routing).

Furthermore, for each sensor, we also calculate the *residual energy*, i.e., the available energy at the end of the simulation. For each scenario we perform 10 simulation runs and we report the mean values and relevant 95% confidence interval of the considered performance metrics.

## V. SIMULATION RESULTS

Figures 2 and 3 show the packet loss as a function of  $R_{eve}$  for AODV and HERA with different  $rTx$  and in case of short ( $t_{eve1} = 60$  s) and long ( $t_{eve2} = 500$  s) event, respectively. Basically, for both the schemes, the packet loss increases with  $R_{eve}$  (and correspondingly with the number of source nodes) due to the increasing number of collisions on the channel. For the same reason, the packet loss is higher as the transmission range increases from  $rTx = 20$  m to  $rTx = 30$  m, due to the higher number of neighbor nodes and higher packet collision probability. However, with HERA routing, the packet loss is very low (from 0% to 5%) with respect to AODV (up to 30% or 80%). In fact, as previously discussed, HERA exploits the IEEE 802.15.4 association procedure for routing, and it

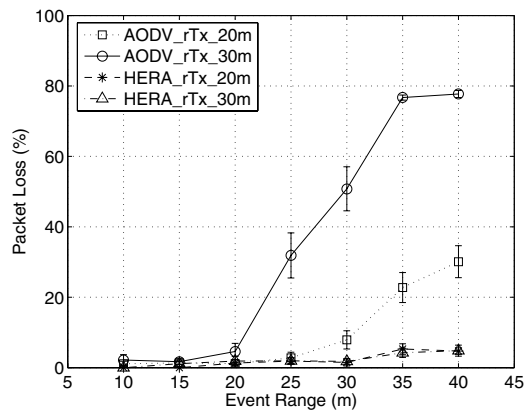


Fig. 2. Packet Loss,  $t_{eve} = 60$  s

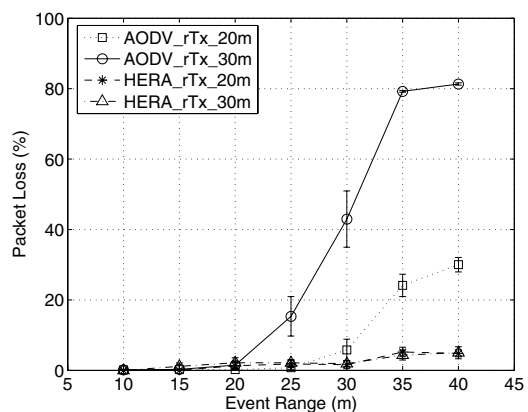


Fig. 3. Packet Loss,  $t_{eve} = 500$  s

does not use extra layer-3 control messages (route reply and route maintenance) or flooding mechanisms (route discovery), which are the main causes of collisions (see a similar issue noticed in mobile ad-hoc networks, known as “the broadcast storm problem” [17] and possible solutions in [18]).

Moreover, from the comparison of Fig. 2 and Fig. 3, it can be noted that the performance of HERA basically does not significantly change for different event duration times, while in the AODV case, packet loss varies for short and long event simulations depending on the  $R_{eve}$  value. Basically, for light network load (i.e.,  $R_{eve} \leq 30$  m), AODV succeeds in converging to a stable routing layout and packet loss mostly occurs during the route discovery phase (due to flooding of route discovery messages). Hence, a shorter event duration triggers more route discovery phases and results in decreased performance with respect to longer events. On the contrary, when the network load increases (i.e.,  $R_{eve} > 30$  m), longer events result in worst performance than short ones. This is due to data packets collisions that occur during the whole duration of the event, and cause routing paths to fail and re-trigger the route discovery mechanism (which boosts the packet loss process).

To better point out the congestion caused by the AODV route discovery process, in Fig. 4 we report the total number of generated route request messages as a function of the event range for different values of  $rTx$ . In the worst case, i.e.,  $rTx = 30$  m, AODV produces about 1100 RREQs to resolve 31 routes from the source nodes to the sink ( $R_{eve} = 40$  m). Moreover, the high load of routing control messages also causes route discovery failures, which result in the nonlinear slope of the curves.

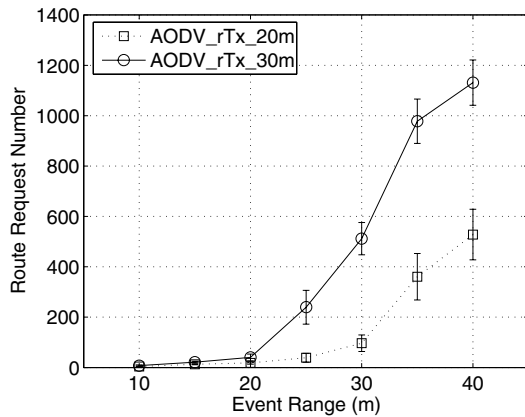


Fig. 4. RREQ exchanged by AODV with  $t_{eve}=60$  s

Figure 5 shows the mean packet delay as a function of  $R_{eve}$  for both the routing schemes. Once again, the very low congestion of HERA results in very low packet delivery delays (few tens of milliseconds). On the other hand, retransmissions at the MAC layer and route resolution failures, caused by collisions, produce higher delays in AODV. In this case, mean delays increase as the radio transmission range and the number of source nodes raise (up to 0.6 s for  $rTx = 30$  m and 0.2 s for  $rTx = 20$  m with 31 source nodes).

Finally, we compared these alternative routing schemes in terms of energy consumption. Figure 6 shows the mean residual energy of the nodes at the end of the simulation as

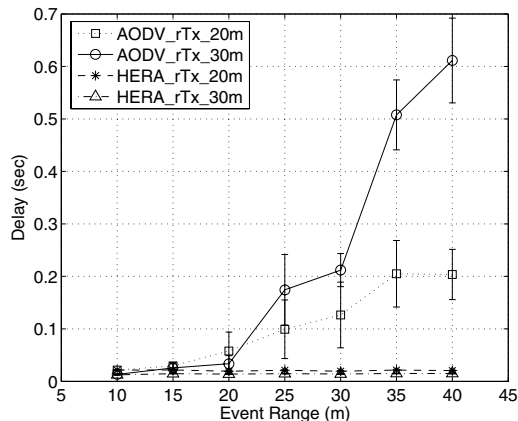


Fig. 5. Mean Delay

a function of  $R_{eve}$ . In accordance with the results discussed so far, lower mean energy consumption is achieved in the HERA case, i.e., lower than 0.5 J, while AODV requires in average 1.5 J and 11.8 J for  $rTx = 20$  m and  $rTx = 30$  m respectively.

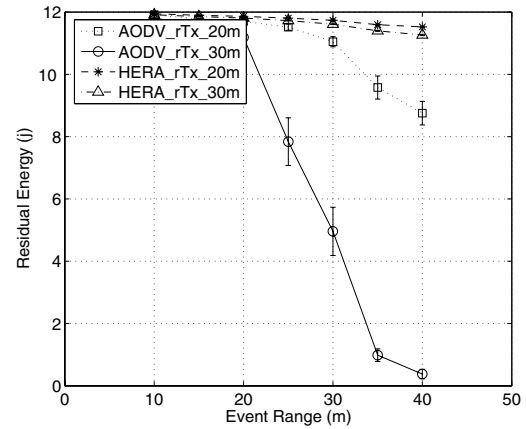


Fig. 6. Residual Energy

It is also important to analyze how energy consumption is distributed among nodes. To this aim, in Figs. 7 and 8, we report the spatial distribution of the residual energy in the network at the end of the simulation, for AODV and HERA, respectively. In these figures, every square represents the level of the residual energy of the node located in the lower left corner of the square. Different intensities of grey represent different energy levels (measured in J), i.e., the lightest reports the lowest residual energy and the darkest shows the highest residual energy.

Since AODV routing paths are more likely to be resolved in less loaded regions of the network (this is a typical characteristic of reactive routing schemes), data paths are not much spatially overlapped. Hence, in this case the residual energy is fairly distributed among all sensors.

On the other hand, in the HERA case data are routed along the parent-child tree, which is closely related to the position of the nodes. Moreover, since source nodes are in the same area, the resolved paths likely include about the same nodes. Therefore, in the HERA case, even if the mean residual energy is higher with respect to AODV, in each simulation run the residual energy is not fairly distributed among the nodes, and is mostly concentrated on a few nodes spatially located between the sources and the sink. The unbalanced energy consumption of highly loaded nodes can lead to early network partitioning.

Finally, it is important to point out that a simplified version of the AODV protocol, AODVjr, has been defined in [19]. AODVjr removes a lot of elements but the essential of AODV and it has nearly the same performance. The main change is that, removing sequence numbers requires the destination to respond to route request messages and so no intermediate nodes may respond. On the contrary AODVjr maintains route discovery flooding and heavy control signaling, which have

been shown to be the main cause of the poor protocol performance. As a consequence, we expect most of our results to hold with AODVjr as well.

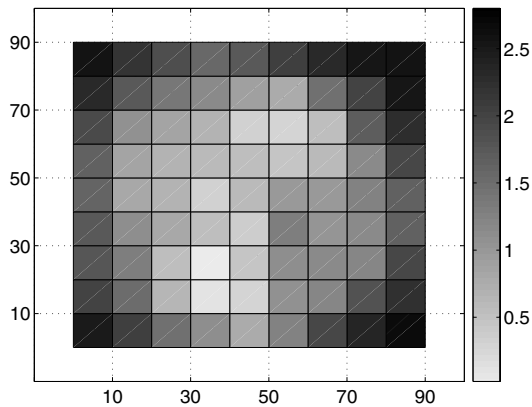


Fig. 7. Energy distribution in AODV (BL)

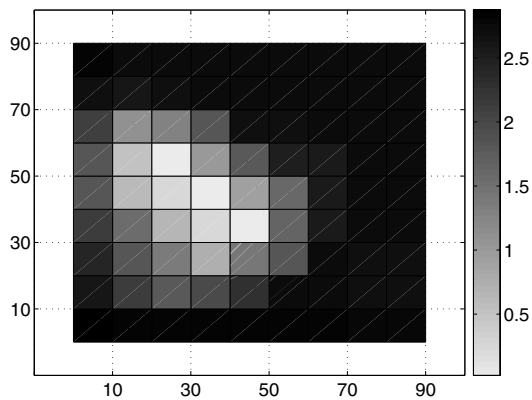


Fig. 8. Energy distribution in HERA (BL)

## VI. CONCLUSIONS

We have compared two routing paradigms proposed by the ZigBee Alliance for IEEE 802.15.4 wireless sensor networks. The first paradigm is the well known Ad-hoc On demand Distance Vector, and the second is a hierarchical routing, which we referred to as HERA. We carried out an extensive simulation analysis to compare HERA and AODV. The proactive scheme HERA, compared with a reactive mechanism, shows better performance with respect to several metrics since, by exploiting the cross-layer interdependencies between the topology formation and the routing mechanisms, it is able to simply set-up routing paths towards a sink.

HERA exploits information exchanged during the network formation and topology update phases, thus avoiding additional routing messages and the associated overhead. Moreover, it shows several performance enhancements with respect

to AODV, such as reduced latency and energy consumption. Finally, it reduces complexity, as it is very easy to implement and does not require a specialized daemon on the host device where it runs. AODV shows in general worse performance. However, since it does not strictly depend on MAC layer procedures, it provides greater flexibility and can be easily extended to account for different route selection metrics. In general, AODV may be selected when the application layer requires high flexibility from the routing mechanism, on the other hand HERA, thanks to its simplicity, is a light routing protocol for simple application scenarios.

## ACKNOWLEDGMENT

This work has been partially supported by the Network of Excellence CRUISE funded by the EU in the framework of the FP6.

## REFERENCES

- [1] *Wireless Medium Access Control (MAC) and Physical Layer (PHY) Specifications for Low Rate Wireless Personal Area Networks (WPANs)*, IEEE Std. 802.15.4, 2003.
- [2] J. Zheng and M. J. Lee, "Will IEEE 802.15.4 make ubiquitous networking a reality?: A discussion on a potential low power, low bit rate standard," *IEEE Communications Magazine*, vol. 27, no. 6, pp. 23–29, 2004.
- [3] E. Callaway, P. Gorday, L. Hester, J. Gutierrez, M. Naeve, B. Heile, and V. Bahl, "Home networking with IEEE 802.15.4: a developing standard for low-rate wireless personal area networks," *IEEE Communications Magazine*, vol. 40, no. 8, pp. 70–77, Aug. 2002.
- [4] J. C. Haartsen and Ericsson Radio Systems B.V., "The Bluetooth Radio System," *IEEE Personal Communications*, pp. 28–36, February 2000.
- [5] J. S. Lee, "An Experiment on Performance Study of IEEE 802.15.4 Wireless Networks," *IEEE*, 2005.
- [6] ZigBee Alliance. [Online]. Available: <http://www.zigbee.org>
- [7] ZigBee Specification, ZigBee Alliance Std., 2005. [Online]. Available: <http://www.zigbee.org>
- [8] Crossbow. [Online]. Available: <http://www.xbow.com>
- [9] Crossbow MICAz Mote Specifications. [Online]. Available: <http://www.xbow.com>
- [10] Crossbow TelosB Mote Specifications. [Online]. Available: <http://www.xbow.com>
- [11] CC2420 Product Information. [Online]. Available: <http://www.chipcon.com>
- [12] C. Perkins, E. Belding-Royer, and S. Das, "Ad hoc on-demand distance vector (aodv) routing," United States, 2003.
- [13] (2002) The The Network simulator-ns-2 website. [Online]. Available: <http://www.isi.edu/nsnam/ns>
- [14] J. Zheng and M. J. Lee. NS2 Simulator for IEEE 802.15.4. [Online]. Available: <http://ees2cy.engr.cny.cuny.edu/zheng/pub/2004>
- [15] The NO Ad-Hoc Routing Agent (NOAH) website. [Online]. Available: <http://icapeople.epfl.ch/widmer/uwb/ns-2/noah/>
- [16] (2006) The Moteiv Corporation Website. [Online]. Available: [http://www.moteiv.com/community/Tmote.Sky\\_Downloads](http://www.moteiv.com/community/Tmote.Sky_Downloads)
- [17] S. Ni, Y. Tseng, Y. Chen, and J. Chen, "The broadcast storm problem in a mobile ad hoc network," in *Proc. Ann. ACM/IEEE Intl. Conf. on Mobile Computing and Networking*, Aug. 1999, pp. 151–162.
- [18] B. Williams and T. Camp, "Comparison of broadcasting techniques for mobile ad hoc networks," in *Proc. 3rd ACM Intl. Symp. on Mobile Ad Hoc Networking and Computing (MobiHoc)*. ACM Press, 2002, pp. 194–205.
- [19] I. D. Chakeres and L. Klein-Berndt, "AODVjr, AODV Simplified," *ACM Mobile Computing and Communications Review*, vol. 6, no. 3, pp. 100–101, 2002.